Solvothermal Synthesis of Gallium and Indium Nitrides Using Lithium Amide

Pietro Chirico and Andrew L. Hector

School of Chemistry, University of Southampton, Highfield, Southampton SO17 1BJ, U. K.

Reprint requests to Dr A. L. Hector. E-mail: a.l.hector@soton.ac.uk

Results of the investigation of the reactions of $GaCl_3$, $InCl_3$ and InI_3 with $LiNH_2$ under solvothermal conditions in benzene, which lead to metal nitrides, are reported. GaN is obtained as a cubic phase or as a mixture of cubic and hexagonal phases, depending on temperature. The effect of the addition of surfactants on the formation of GaN was explored. InN products were always contaminated with indium metal, even at low reaction temperatures. The addition of excess $LiNH_2$ or the use of InI_3 instead of $InCl_3$ gave products with less In metal.

Key words: Gallium Nitride, Indium Nitride, Nanocrystal, Solvothermal Synthesis

Introduction

Gallium and indium nitrides are important optoelectronic materials with band gaps ranging from 0.7 eV in InN to 3.4 eV in GaN. GaN is especially relevant as, with the introduction of suitable dopants or in solid solution with InN, its band gap can be varied to emit light from the UV to the IR region. When used in electronic devices, these nitrides are typically produced using MOVPE or MOCVD techniques [1]. They have also been prepared in powdered form by high-temperature ammonolysis [2] or metal amide decomposition [3], and as nanoparticle colloids by decomposition of molecular precursors in hot solvents [4]. Solvothermal synthesis is gradually developing into a useful technique to produce metal nitrides in nanocrystalline form [5], including anisotropic particles. Typically the reagents are those that have previously been used in solid-state metathesis, especially metal chlorides and Li_3N or NaN_3 [6]. Nanocrystalline GaN has been produced from Li_3N and $GaCl_3$ in benzene at 280 °C [7] as nanocrystals of $\sim$ 30 nm diameter. Under these conditions a mixture of hexagonal and rocksalt-type GaN was produced. This was surprising as rocksalt-type GaN is normally only found at high pressure [8]. $GaCl_3$ and NaN_3 react in toluene or THF at 260 °C, producing a poorly crystalline product [9], but on annealing to 750 °C hexagonal GaN crystals of $\sim$ 8 nm size were produced. Hexagonal GaN has also been prepared using solvothermal reactions between Ga cupferron or $GaCl_3$ and $(Me_3Si)_2NH$ (HMDS) [10]. In this work the authors added a surfactant (*N*-cetyltrimethylammonium bromide) and obtained capped nanoparticles. Solvothermal synthesis of InN has been achieved *via* reactions of $InCl_3$ with Li_3N in xylene [11] or of InI_3 with $NaNH_2$ in benzene, both at around 250 °C [12]. Another report showed the reactions between $InBr_3$ and NaN_3 in toluene or hexadecane at $\sim$ 280 °C to produce 10 nm hexagonal InN crystallites, with some evidence of cubic InN at lower temperatures [13].

Recently we have been studying the reactions of transition metal chlorides with $LiNH_2$ and NH_3 under solvothermal conditions. We have found that these are effective methods to produce nanocrystalline nitride materials with metals of groups 4, 5 and 6 [14]. In some cases, most extensively with Ta, we have found that nanorods can also be grown under these conditions. In the work described in this paper we examined reactions between gallium and indium chlorides, and indium iodide, with $LiNH_2$ under similar conditions. We also investigated the effect of the addition of surfactants on the synthesis of GaN.

Experimental Section

All preparations were carried out under anaerobic conditions using either glove box or Schlenk line techniques for sample loading and handling. Benzene was distilled from Na, methanol from $NaOCH_3$, and hexadecylamine (HDA) from BaO. $GaCl_3$ (99.999 %), $InCl_3$ (99.999 %), InI_3 (99.998 %) and *N*-cetyltrimethylammonium bromide (CTAB; > 99 %) were purchased from Aldrich and used as supplied. Ammo-

nia (Air Products) was distilled from a sodium/ammonia solution before use. $LiNH_2$ was synthesised by reacting 1.6 M ^{n}BuLi in hexane (Aldrich) with excess distilled ammonia at -78 °C, filtering, and drying the product *in vacuo*.

All syntheses were performed in a 75 cm^3 autoclave (Parr 4740CH). Typically, 0.6 g of metal chloride was placed in the silica liner and covered with 15 cm^3 of benzene. A stoichiometric amount of $LiNH_2$, calculated to balance the lithium and chloride components of the reaction mixture, was added. The autoclave was heated at the temperatures detailed later, typically for 24 h. After cooling to r.t., the autoclave was opened, and the mixture was transferred to a Schlenk tube inside the glove box. The solid was collected by filtration, washed with dry methanol three times to remove the LiCl by-product, and dried *in vacuo*.

Powder X-ray diffraction (PXD) measurements were performed on a Siemens D5000 diffractometer using $CuK_{\alpha1}$ ($\lambda = 1.5406$ Å) radiation. The phases present were identified by comparison with the JCPDS database [15] and patterns refined using the GSAS package [16]. Crystallite sizes were obtained using the Scherrer formula. Transmission electron microscopy (TEM) was carried out with a Hitachi 7000 (75 kV) instrument. Samples were prepared by ultrasound dispersal in toluene, followed by deposition on carbon-coated Cu grids. IR spectra were recorded from CsI disks using a Perkin Elmer Spectrum 100 instrument. TGA data were collected with a Mettler Toledo TGA851e under flowing high-purity nitrogen with a heating rate of 10°/min. C, H, N combustion analyses and Schöniger flask combustion analysis of chlorine content were carried out by Medac Ltd. (Egham, Surrey, UK).

Results and Discussion

Reactions of gallium chloride with lithium amide

The solvothermal route to GaN nanocrystals in benzene using $LiNH_2$ as the nitrogen source was envisaged to proceed as follows:

$$GaCl_3 + 3 LiNH_2 \rightarrow GaN + 3 LiCl + 2 NH_3$$

Samples were prepared at temperatures in the range 250–450 °C. At 250 °C zinc blende-type (cubic) GaN was obtained, whereas at higher temperatures a mixture of the zinc blende- and the wurtzite-type (hexagonal) phases formed (Fig. 1). The feature below 25° in the patterns collected from samples made at 250–350 °C is due to some amorphous content, whereas the peak at 26° is due to pyrolytic carbon produced by solvent decomposition during the reactions. The 220 reflection in the cubic phase does not overlap with other peaks and was used to calculate a lattice parameter of $a = 4.46$ Å and an average crystallite size

Table 1. The products from reactions of $GaCl_3$ and $LiNH_2$. Analyses are accurate to ± 0.3 %.

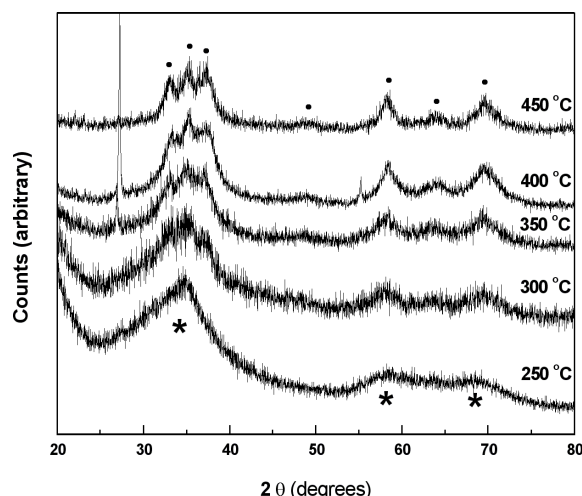| Temperature (°C)	Composition	% C	% N	% H
450	$GaN_{0.69}C_{0.16}$	2.4	11.9	0.8
400	$GaN_{0.68}C_{0.26}$	3.9	11.5	1.1
350	$GaN_{0.69}C_{0.20}$	2.9	11.8	1.3
300	$GaN_{0.70}C_{0.13}$	2.0	12.1	1.6
250	$GaN_{0.70}C_{0.36}$	5.1	11.7	2.1

Fig. 1. PXD patterns ($CuK_{\alpha1}$) of the samples prepared at different reaction temperatures from $GaCl_3$ and $LiNH_2$ (● = reflection positions for wurtzite-type GaN; * = positions for the 111, 220 and 311 reflections of zinc blende-type GaN; the 200 and 222 peaks are responsible for the asymmetry of the 111 and 311 peaks).
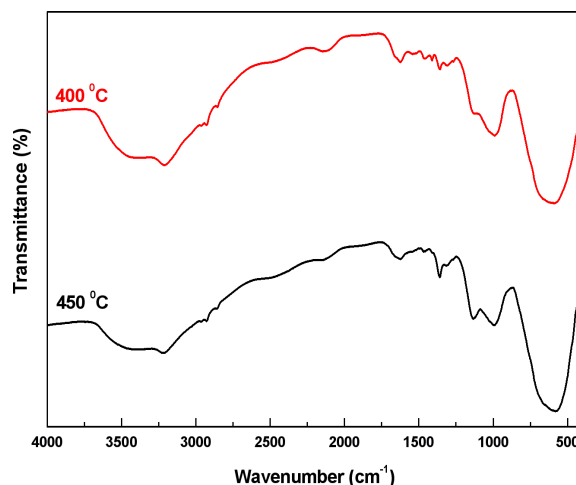

Fig. 2. IR spectra of GaN produced from $GaCl_3$ and $LiNH_2$ at 400 and 450 °C.

of 1.8 nm. Literature reports of the lattice parameters of GaN range from 4.36–4.47 Å [16].
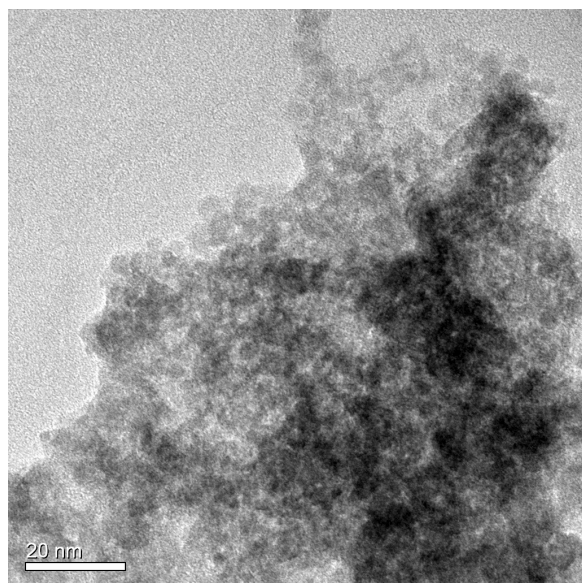
Fig. 3. TEM image of GaN prepared from $GaCl_3$ and $LiNH_2$ at 300 °C.

Combustion analysis revealed nitrogen-deficient GaN samples with significant carbon and hydrogen content (Table 1). A small amount of chlorine ($< 5\%$) was also found in the products. The IR spectra (Fig. 2) show a broad Ga-N stretch around 600 cm^{-1} (double peak due to A_1+E_1 modes), significant ν(N-H) and weak ν(C-H) bands [17]. The mechanism of GaN formation most likely involves metathesis reactions that produce Ga-NH$_2$ groups that then condense with neighbouring Ga centres. Hence the presence of residual NH groups in the products at these relatively mild temperatures is not surprising. The decomposition of solvent to produce carbon is less expected. TEM showed regular-shaped crystallites with particle sizes below 5 nm (Fig. 3). All of the samples studied had significant aggregation of these crystallites.

Reactions between GaCl$_3$ and LiNH$_2$ in the presence of hexadecylamine

The use of surfactants to control the particle size and prevent the agglomeration of nanoparticles is common, and there is one reported example of the production of capped GaN nanocrystals under solvothermal conditions by adding CTAB [10]. Hence reactions analogous to those described above were tried with added hexadecylamine. Various amounts of HDA were added to reactions between GaCl$_3$ and LiNH$_2$ in ben-

Table 2. Products identified from the reactions of $GaCl_3$ and $LiNH_2$ with added HDA. Combustion analyses are accurate to $\pm 0.3\%$.

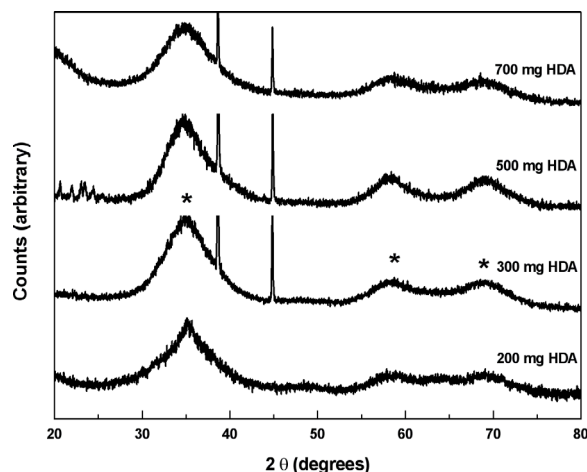| Composition	HDA (mg)	% C	N	H	Crystallite size (nm)	a (Å)
$GaN_{0.17}C_{0.93}$	200	13.4	2.9	3.4	2.0	4.48
$GaN_{0.27}C_{1.25}$	300	16.9	4.3	3.9	2.0	4.46
$GaN_{0.50}C_{2.00}$	500	23.8	7.0	4.8	1.8	4.48
$GaN_{0.76}C_{2.73}$	700	28.9	9.5	5.4	1.8	4.48

Fig. 4. XRD patterns of samples prepared from $GaCl_3$ and $LiNH_2$ at 250 °C with different amounts of HDA. The 111, 220 and 311 GaN reflections are marked by asterisks. Two aluminium peaks resulting from the sample holder are visible in some data sets at 38 and 44°.

zene at 250 °C in an attempt to produce capped particles. PXD data identified all of the products as cubic GaN (Fig. 4). The addition of small amounts of HDA led to a small increase in the crystallite size and a reduction in the amorphous content of the samples. When 300 or 500 mg of HDA was added, the PXD patterns showed very little amorphous scattering. This change suggests that HDA becomes involved in the formation of GaN, possibly reacting more readily with the GaCl$_3$ in solution than does the solid LiNH$_2$. Metal primary amides can self-condense to produce bridging imide groups. This is chemistry that we have used in sol-gel processing of TiN [18]. Addition of further HDA, however, resulted in the reappearance of amorphous features in the diffraction patterns and further broadening of the reflections. The lattice parameters of these samples are a little higher than those of samples produced without HDA and also slightly higher than the normal range of literature values. Carbon incorporation into nitride structures typically results in an increase in the lattice parameter.
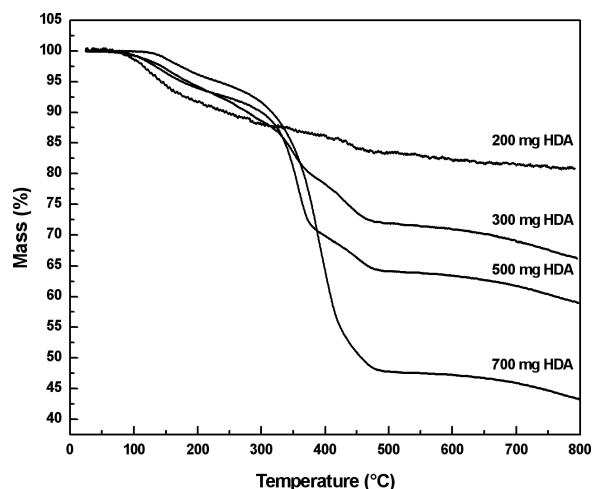
Fig. 5. TGA of samples produced from GaCl$_3$ and LiNH$_2$ with different amounts of HDA.

Carbon incorporation directly into the GaN structure is also consistent with the microanalysis results (Table 2) that show low nitrogen contents (GaN contains 16.7 % N) in these samples. The C, H and N contents all increase as more HDA is added to the reactions, showing that it is carried through to the products. The IR spectra showed significant sharp ν(C-H) and broad ν(N-H) bands, and also broad bands in the ν(Ga-N) region around 600 cm^{-1} [19]. TGA traces (Fig. 5) showed a feature with an onset around 100 °C that could be due to loss of benzene that was dissolved in the HDA and hence not removed when the samples were dried *in vacuo*. Two further major features are then observed with onsets of around 300 and 400 °C. It is likely that the lower temperature mass loss is unbound HDA and the higher temperature one is surface-bound HDA, as the sample with only 200 mg HDA only shows the higher temperature feature. TEM images of these samples were somewhat indistinct, probably due to the HDA coating the spaces between particles, but it was apparent that there was a similar level of aggregation to that observed without HDA.

Reactions between GaCl$_3$ and LiNH$_2$ in the presence of N-cetyltrimethylammonium bromide

CTAB was previously used to cap GaN particles grown in solvothermal reactions between gallium cupferron and hexamethyldisilazane in toluene [10]. Addition of CTAB to the reactions between GaCl$_3$ and LiNH$_2$ resulted in PXD patterns similar to those observed with added HDA (Fig. 6). Small quantities re-

Table 3. Compositions and structural data for products of the reactions of GaCl$_3$ and LiNH$_2$ using different amounts of CTAB. Combustion analyses are accurate to ± 0.3 %.

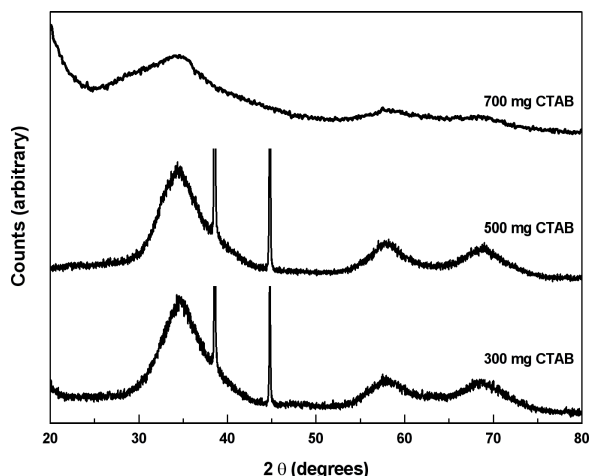| Composition	CTAB (mg)	% C	% N	% H	Crystallite size (nm)	a (Å)
GaN$_{0.73}$C$_{0.37}$	300	5.3	12.1	2.2	1.8	4.49
GaN$_{0.61}$C$_{0.37}$	500	5.3	10.3	2.3	2	4.51
	700	–	–	–	1.8	4.50

Fig. 6. PXD patterns of the products from the reactions of GaCl$_3$ with LiNH$_2$ using different amounts of CTAB. Sharp peaks at 38 and 44° are due to the Al sample holder.
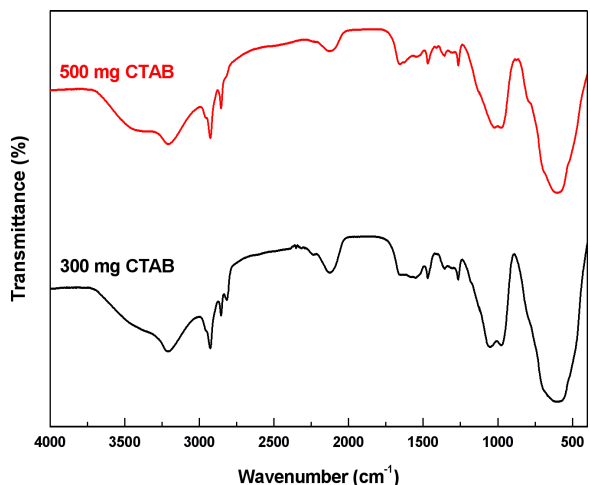

Fig. 7. IR spectra of the products of reactions of GaCl$_3$ with LiNH$_2$ using different amounts of CTAB.

sulted in a reduction in the amorphous content of the samples, but with larger additions the amorphous features returned to the PXD patterns. Lattice parameters (Table 3) were slightly high, again probably reflecting some carbon incorporation. Interestingly
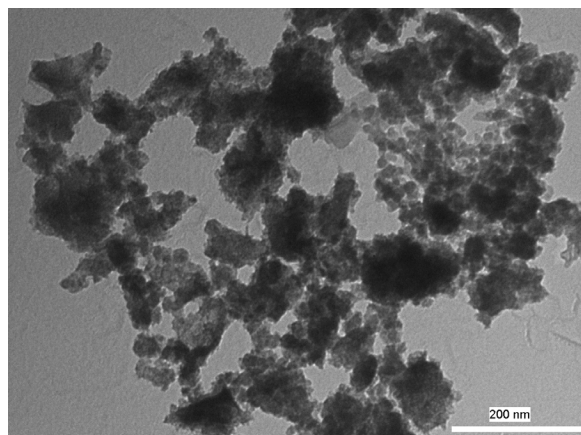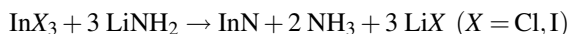
Fig. 8. TEM image of GaN produced from $GaCl_3$ and $LiNH_2$ with 500 mg added CTAB.
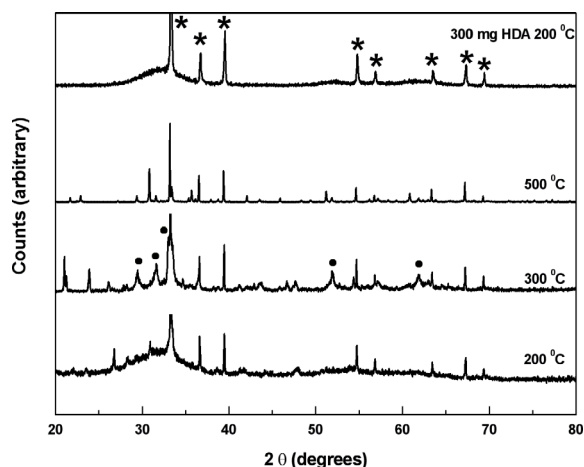

Fig. 9. XRD patterns of samples from solvothermal reactions of $InCl_3$ with $LiNH_2$ carried out at different temperatures. ● = hexagonal InN; * = In metal.

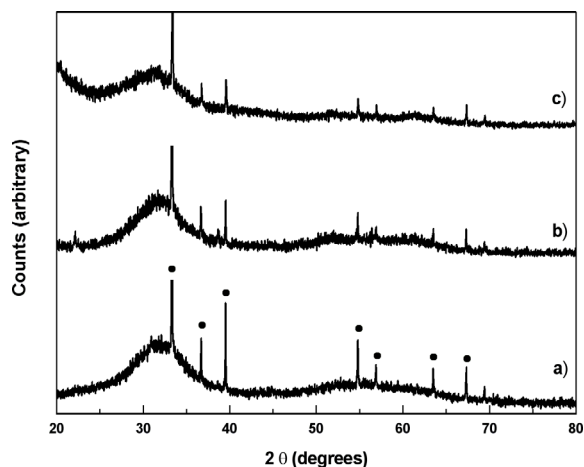the composition of the products varied less with the amount of CTAB, and the nitrogen content was higher-presumably the higher solubility of CTAB than that of HDA in benzene and methanol allows more efficient removal of the former. The TGA traces were also very similar for samples made with different amounts of CTAB. IR spectra (Fig. 7) contained a strong ν(Ga-N) band at ~ 600 cm^{-1} and features corresponding to ν(C-H) and ν(N-H), the relative strength of these features also being very similar however much CTAB was added to the reaction mixture. Disappointingly TEM images still showed significant aggregation in these samples, though there was some evidence of individual particles (Fig. 8).

Reactions of indium chloride and iodide with lithium amide

Due to its low thermal stability [19, 20], InN is more difficult to synthesise than GaN. Our aim was the preparation of InN by methods analogous to those described above for GaN:

$$InX_3 + 3\,LiNH_2 \rightarrow InN + 2\,NH_3 + 3\,LiX \;\; (X = Cl, I)$$

Reactions of $InCl_3$ with $LiNH_2$ resulted in samples containing In metal, even at temperatures well below the decomposition temperature of InN (Fig. 9). After reaction at 200 °C broad reflections are observed in addition to the In peaks, and these closely resemble the zinc blende-type GaN peaks. On raising the temperature, sharper peaks attributable to wurtzite-type (hexagonal) InN are observed, and on raising the temperature further to 500 °C only In metal is observed.

Fig. 10. XRD patterns of InN obtained from $InCl_3$ and $LiNH_2$ at 200 °C using: a) a 20 % excess of $LiNH_2$, b) a 50 % excess of $LiNH_2$, and c) a 100 % excess of $LiNH_2$ (● marks peak positions attributable to In metal).

Addition of HDA to the low-temperature (200 °C) reaction did appear to reduce the amount of In in the samples, but significant amounts were still formed.

An obvious way to reduce the amount of indium metal by-products in these reactions would be to increase the overall nitrogen content of the reaction mixture. Hence the effect of using an excess of the nitrogen source reagent, $LiNH_2$, was investigated. Fig. 10 shows the effect of excess $LiNH_2$. A small excess, 20 %, resulted in a reduction in the amount of In in the zinc blende-type InN products, but further additions of $LiNH_2$ resulted in no further improvement and,
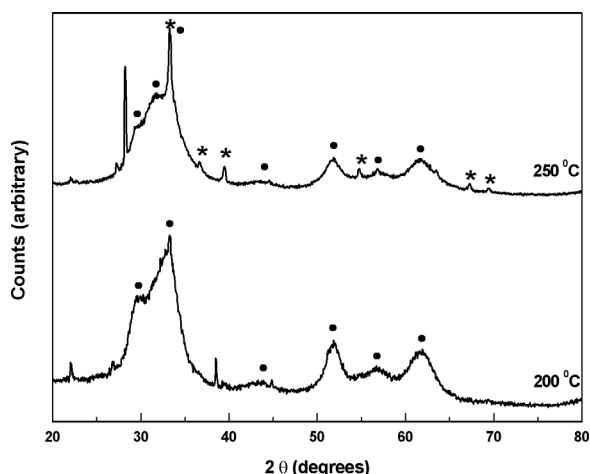
Fig. 11. XRD patterns of InN obtained using InI_3 and $LiNH_2$ at different temperatures. ● = wurtzite-type InN, * = In metal.

at 100 % excess, amorphous scattering was observed in the diffraction pattern. Another option that has been reported by others [12] is the synthesis of InN from InI_3 instead of $InCl_3$. InI_3 has a higher degree of covalent bonding than $InCl_3$ and this has been argued as the reason why In^{3+} from InI_3 is less liable to be reduced to elemental indium. Reactions of InI_3 with $LiNH_2$ resulted in wurtzite-type InN (Fig. 11). Some indium was

still also present even at 200 ℃, and the amount increased at 250 ℃.

Conclusions

Solvothermal reactions of $GaCl_3$ with $LiNH_2$ are an effective method to produce nanocrystalline GaN. At 250 ℃, GaN forms with the zinc blende structure type, whereas at higher temperatures a mixture of zinc blende- and wurtzite-type phases forms. Addition of small amounts of hexadecylamine or *N*-cetyltrimethylammonium bromide surfactants to the low-temperature reactions results in an increase in crystallinity, but aggregation of the particles is not fully inhibited. The analogous reactions with $InCl_3$ produces InN, but this was contaminated with In metal even at reaction temperatures as low as 200 ℃. Use of excess $LiNH_2$, or substitution of InI_3 for $InCl_3$, reduces the amount of In in the products, but does not eliminate it entirely.

[1] D. A. Neumayer, J. G. Ekerdt, *Chem. Mater.* **1996**, *8*, 9; H. Monkoc, S. Strilé, G. B. Gao, M. E. Lin, B. Sverdlov, M. Burns, *J. Appl. Phys.* **1994**, *76*, 1363; B. Garni, J. Ma, N. Perkins, J. Liu, T. F. Kuech, M. G. Lagally, *Appl. Phys. Lett.* **1996**, *68*, 1380; S. D. Lester, F. A. Ponce, M. G. Craford, D. A. Steigerwald, *Appl. Phys. Lett.* **1995**, *66*, 1249; F. A. Ponce, D. A. Bour, W. Götz, P. J. Wright, *Appl. Phys. Lett.* **1996**, *68*, 57.

[2] A. P. Purdy, *Chem. Mater.* **1999**, *11*, 1648; J. Jegier, S. McKernan, A. P. Purdy, W. L. Gladfelter, *Chem. Mater.* **2000**, *12*, 1003; D. R. Ketchum, J. W. Kolis, *J. Cryst. Growth* **2001**, *222*, 431.

[3] J. F. Janik, R. L. Wells, J. L. Coffer, J. V. St. John, W. T. Pennington, G. L. Schimek, *Chem. Mater.* **1998**, *10*, 1613; J.-W. Hwang, J. P. Campbell, J. Kozubowski, S. A. Hanson, J. F. Evans, W. L. Gladfelter, *Chem. Mater.* **1995**, *7*, 517.

[4] O. I. Mícíc, S. P. Ahrenkiel, D. Bertram, A. J. Nozik, *Appl. Phys. Lett.* **1999**, *75*, 478.

[5] B. Mazumder, A. L. Hector, *J. Mater. Chem.* **2009**, *19*, 4673; G. Demazeau, *J. Mater. Sci.* **2008**, *43*, 2104.

[6] J. B. Wiley, R. B. Kaner, *Science* **1992**, *255*, 1093; J. C. Fitzmaurice, A. Hector, I. P. Parkin, *Polyhedron* **1993**,

12, 1295; J. C. Fitzmaurice, A. L. Hector, I. P. Parkin, *J. Chem. Soc., Dalton Trans.* **1993**, 2435; A. Hector, I. P. Parkin, *J. Chem. Soc., Chem. Commun.* **1993**, 1095; E. G. Gillan, R. B. Kaner, *Chem. Mater.* **1996**, *8*, 333; E. G. Gillan, R. B. Kaner, *Inorg. Chem.* **1994**, *33*, 5693; A. L. Hector, I. P. Parkin, *Polyhedron* **1995**, *14*, 913.

[7] Y. Xie, Y. Qian, W. Wang, S. Zhang, Y. Zhang, *Science* **1996**, *272*, 1926.

[8] C. Falter, M. Klenner, Q. Chen, *Phys. Rev. B* **1993**, *48*, 16690.

[9] Y. Zhang, J. Liu, R. He, Q. Zhang, X. Zhang, J. Zhu, *Chem. Phys. Lett.* **2002**, *360*, 579.

[10] K. Sardar, C. N. R. Rao, *Adv. Mater.* **2004**, *16*, 425.

[11] C. Wu, T. Li, L. Lei, S. Hu, Y. Liu, Y. Xie, *New J. Chem.* **2005**, *29*, 1610.

[12] Y.-J. Bai, Z.-G Liu, X.-G. Xu, D.-L Cui, X.-P. Hao, X. Feng, Q.-L Wang, *J. Cryst. Growth* **2002**, *241*, 189.

[13] J. Choi, E. G. Gillan, *J. Mater. Chem.* **2006**, *16*, 3774.

[14] B. Mazumder, A. L. Hector, *J. Mater. Chem.* **2008**, *18*, 1392; B. Mazumder, P. Chirico, A. L. Hector, *Inorg. Chem.* **2008**, *47*, 9684; P. Chirico, A. L. Hector, B. Mazumder, *Dalton Trans.* **2010**, *39*, 6092.

[15] PCPDFWIN (version 2.4), Powder Diffraction File,

International Center for Diffraction Data, Swarthmore, PA (USA) **2003**.

[16] A. C. Larson, R. B. Von Dreele, General Structure Analysis System (GSAS), report LAUR 86-748, Los Alamos National Laboratory **2004**; B. H. Toby, *J. Appl. Crystallogr.* **2001**, *34*, 210.

[17] G. Socrates, *Infrared and Raman Characteristic Group Frequencies*, Wiley **2006**, pp. 109 – 111.

[18] B. M. Gray, S. Hassan, A. L. Hector, A. Kalaji, B. Mazumder, *Chem. Mater.* **2009**, *21*, 4210; A. W. Jackson, A. L. Hector, *J. Mater. Chem.* **2007**, *17*, 1016.

[19] S. Porowski, I. Grzegory, *EMIS Datarev. Ser.* **1994**, *11*, 82.

[20] S. Krukowski, A. Witek, J. Adamczyk, M. Bockowski, I. Grzegory, B. Lucznik, G. Nowak, M. Wroblewski, A. Presz, S. Gierlotka, S. Stelmach, B. Palosz, S. Porowski, P. Zinn, *J. Phys. Chem. Solids* **1998**, *59*, 289.